Article

Quintessential Water from Cosmic Dust: A Possible Origin of Dark Matter, Dark Energy, and Life in the Universe

Keith Johnson *

Posted Date: 16 November 2023

doi: 10.20944/preprints202311.1084.v1

Keywords: Dark Matter; Dark Energy; Life; Cosmic Dust; Water Nanoclusters

Article

Quintessential Water from Cosmic Dust: A Possible Origin of Dark Matter, Dark Energy, and Life in the Universe

Keith Johnson

Massachusetts Institute of Technology, Cambridge, MA 02139; kjohnson@mit.edu

Abstract: The creation of protonated water nanoclusters from amorphous water-ice under laboratory conditions suggests the possible ejection of such nanoclusters from ubiquitous amorphous water-ice-covered cosmic dust to interstellar space. The quantum properties of these quintessential water entities introduce a tantalizing prospect that bridges the origins of dark matter, dark energy, and life in the universe. The quantum-entangled diffuse Rydberg electronic states inherent to cosmic water nanoclusters make them plausible candidates for baryonic dark matter. Moreover, they exhibit the capacity to absorb, through the microscopic dynamical Casimir effect, virtual photons originating from zero-point-energy vacuum fluctuations occurring above the water-nanocluster vibrational frequency cutoff. This selective interaction leaves only vacuum fluctuations below these frequencies with gravitational significance, cancelling the vacuum-energy catastrophe and yielding a shared genesis for dark matter and dark energy. Moreover, this theory extends its implications to the origins of life itself, proposing that RNA protocells on Earth and habitable exoplanets may have emerged from the interactions between cosmic water nanoclusters and prebiotic organic molecules, thus yielding an anthropic narrative. Collectively, these findings coalesce into a cosmological framework depicting a cyclic universe, with cosmic water nanoclusters constituting a quintessence scalar field, instead of adhering to the multiverse concept based on cosmic inflation theory. Recent observations of CMB birefringence support this quintessence.

Keywords: Dark Matter; Dark Energy; Life; Cosmic Dust; Water Nanoclusters

1. Introduction

In the standard framework of Big Bang cosmology, the matter and energy composition of our universe is governed by two enigmatic entities: *dark matter*, a nonbaryonic substance with an unknown nature, and *dark energy*, a strange negative-pressure field. Despite over three decades of searching, proposed exotic elementary particles such as weakly interacting massive particles (WIMPs) and AXIONS have yet to materialize in experimental observations. Similarly, predictions of WIMPs stemming from supersymmetry theory have not been realized in the CERN LHC ATLAS detector. Dark energy, responsible for the accelerating expansion of the universe, is typically regarded as a distinct challenge from dark matter and is associated with fluctuations of the zero-point energy of the cosmic vacuum. Moreover, quantum field theory predicts a vacuum energy density that exceeds the observed value by as much as a staggering factor of 10^{120}, known as the *cosmological constant problem* [1]. In this paper, I propose that water nanoclusters, ejected from amorphous water-ice enveloping ubiquitous cosmic dust, as simulated in the laboratory [2], when excited to their diffuse Rydberg electronic states, may serve as plausible candidates for *baryonic* dark matter [3]. The cutoff terahertz (THz) vibrational frequencies of these water nanoclusters align closely with the $\nu_c \cong$ 1.7 THz cutoff frequency of vacuum fluctuations, proposed by Beck and Mackey [4] to account for the small value of vacuum energy and the cosmological constant. I suggest that cosmic water nanoclusters can also harness high-frequency vacuum zero-point-energy virtual photons through the microscopic dynamical Casimir effect [5], leaving only the low-frequency ones to exert gravitational influence, thereby cancelling the infamous *vacuum-energy catastrophe* or cosmological constant problem [1]. Finally, it is worth noting that approximately seventy percent of our body weight

 doi:10.20944/preprints202311.1084.v1

consists of water, including water nanoclusters known as "structured water" [6]. This fact adds scientific and philosophical credence, rooted in the simplest anthropic principle, to the hypothesis that water nanoclusters, distributed as a low-density "quintessence dark fluid" throughout the universe, might represent a plausible shared source of both dark matter and dark energy, alongside or instead of yet-to-be-discovered exotic elementary particles like WIMPS and AXIONS, as well as being the key precursor, along with prebiotic carbon-based molecules, to life's origin in the *RNA World* [7].

2. Cosmic Water Nanoclusters: Electronic Structure and Terahertz (THz) Vibrations

The continued non-detection of WIMP and AXION elementary particles, which were prime candidates for dark matter, raises a fundamental question: Could water nanoclusters hold clues to understanding these cosmic enigmas? It is essential to recognize the predominant role of hydrogen and oxygen - the constituents of water - in our universe. Both are among the most abundant and chemically active. Intriguingly, water vapor plays a pivotal role during the early phases of star creation. In these regions, water acts as a significant oxygen reservoir, ensuring the effective cooling of the surrounding gas, which is a crucial process in star evolution [8]. In fact, regions such as the Orion nebula are known to generate immense amounts of water daily, much more than the volume of Earth's oceans [9]. Moreover, the discovery of massive reservoirs of water, associated with high-redshift quasars, twelve or more billion light-years from Earth, underscores the widespread presence of water in the universe [10]. Such quasars, housing astounding masses of water vapor, are indicative of water's abundance even in remote cosmic locales. Furthermore, recent studies suggest that during the universe's infancy - the initial billions of years post Big Bang - water could have been quite widespread [11]. Closer to home, stable water nanoclusters arise in the atmosphere because of hydrogen bonding between water molecules [12]. A plausible mechanism for the formation of these nanoclusters in the cosmos is cosmic-ray-induced direct ejection from amorphous ice covering cosmic dust grains, as observed under laboratory conditions [2]. These grains, which are prevalent in interstellar clouds, owe their existence to supernovae explosions [13]. The cosmic-ray-induced ionization of H_2 molecules adsorbed on amorphous water-ice, namely, $H_2^+ + nH_2O$ + grain $\rightarrow$ $H_3O^+(H_2O)_{n-1}\uparrow$ + grain, is another proposed scenario for the ejection of protonated water nanoclusters to interstellar space [14]. These ionized water nanoclusters, owing to their oscillating electric dipole moments, are linked to the observed THz emissions from water vapor under intense UV radiation [15] and thus should be stable under similar cosmic radiation. Interestingly, $H_3O^+(H_2O)_{20}$ or its equivalent protonated form, $(H_2O)_{21}H^+$ is notably stable under vacuum conditions. This "magic-number" structure can be visualized as a hydronium ion, H_3O^+ encased by a pentagonal dodecahedral assembly of twenty water molecules (Figure 1d). The stability of this unique structure may have cosmic implications, as suggested by the recent observation of interstellar hydronium [16]. Spectroscopic identification of larger protonated cosmic water nanoclusters is a challenge, but crucial for confirming their presence and understanding their possible role in cosmic phenomena.

Preprints (www.preprints.org) | NOT PEER-REVIEWED | Posted: 16 November 2023 doi:10.20944/preprints202311.1084.v1

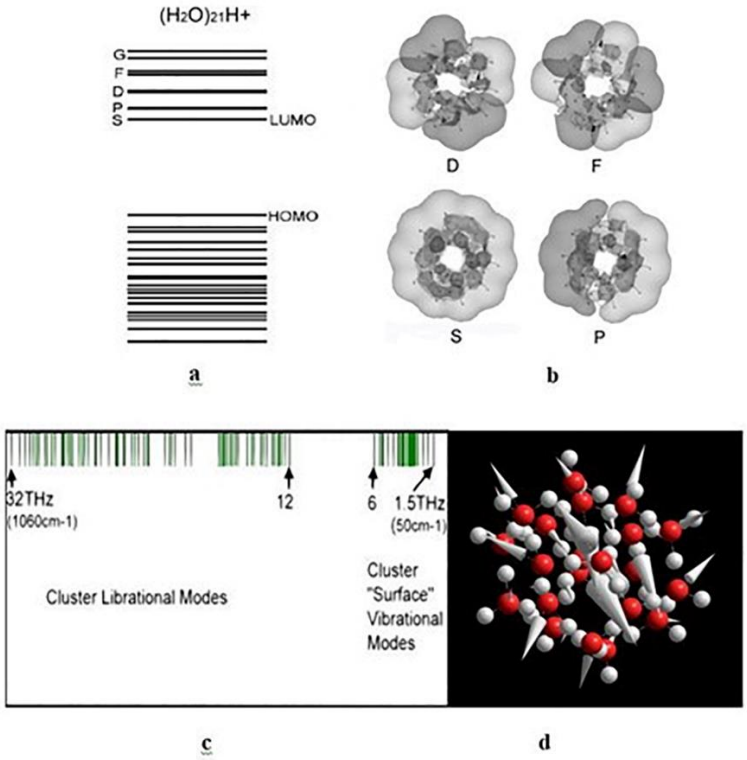

Figure 1. Molecular-orbital energy levels, wavefunctions, and vibrational modes of the protonated $(H_2O)_{21}H^+$ cluster, calculated using the SCF-Xα-Scattered-Wave density-functional method (Reference 17). **a.** Cluster molecular-orbital energy levels. The HOMO-LUMO energy gap is approximately 3 eV. **b.** Wavefunctions of the lowest unoccupied cluster molecular orbitals. **c.** THz vibrational spectrum. **d.** Lowest-frequency THz vibrational mode and relative vibrational amplitudes. The vectors show the directions and relative amplitudes for the oscillation of the hydronium $(H_3O)^+$ oxygen atom coupled to the O–O–O "bending" motions of the cluster "surface" oxygen atoms.

Figure 1 illustrates the ground-state molecular-orbital energies, wavefunctions, and vibrational modes of the protonated pentagonal dodecahedral water cluster, $(H_2O)_{21}H^+$. These results were obtained using the SCF-Xα-Scattered-Wave density-functional method, a collaborative development by the author [17]. Molecular dynamics simulations confirm the stability of the cluster at temperatures exceeding 100°C, with minimal changes. Similar calculations were performed for the neutral pentagonal dodecahedral water cluster, $(H_2O)_{20}$, and its arrays, revealing THz vibrational modes, as depicted in Figures 2 and 3.

Preprints (www.preprints.org) | NOT PEER-REVIEWED | Posted: 16 November 2023 doi:10.20944/preprints202311.1084.v1

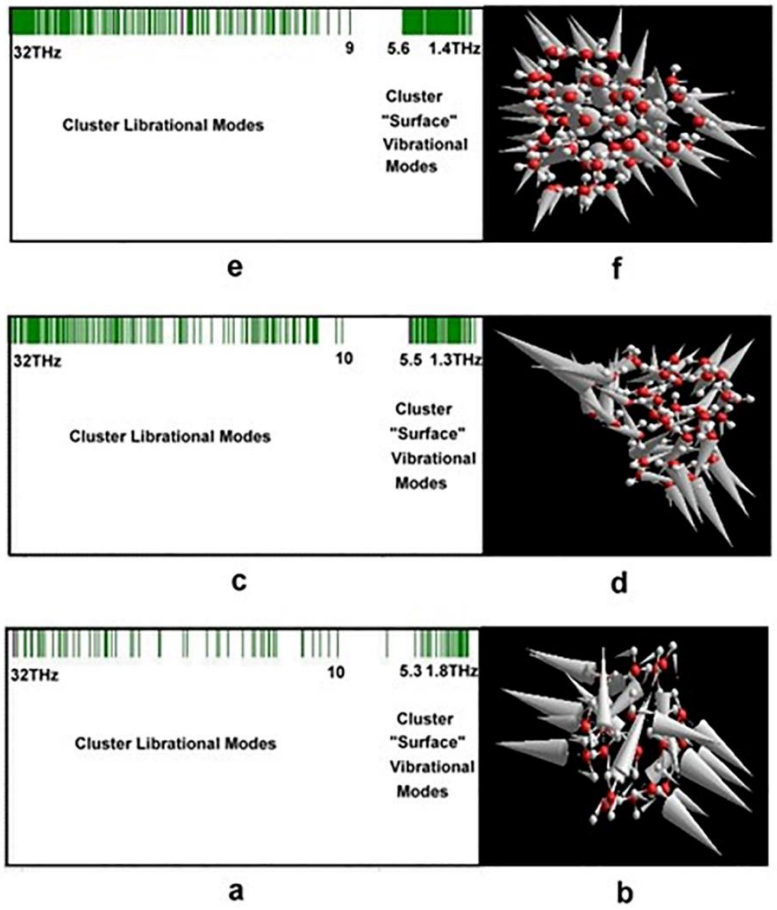

Figure 2. a. THz vibrational spectrum of a pentagonal dodecahedral $(H_2O)_{20}$ cluster calculated using the SCF-Xα-Scattered-Wave density-functional method (Reference 17). **b.** Lowest-frequency THz vibrational mode and relative vibrational amplitudes. **c.** Calculated THz vibrational spectrum of a stable array of three dodecahedral water clusters. **d**. Lowest-frequency THz vibrational mode. **e.** THz vibrational spectrum of a stable array of five dodecahedral water clusters. **f.** Lowest-frequency THz vibrational mode.

Preprints (www.preprints.org) | NOT PEER-REVIEWED | Posted: 16 November 2023 doi:10.20944/preprints202311.1084.v1

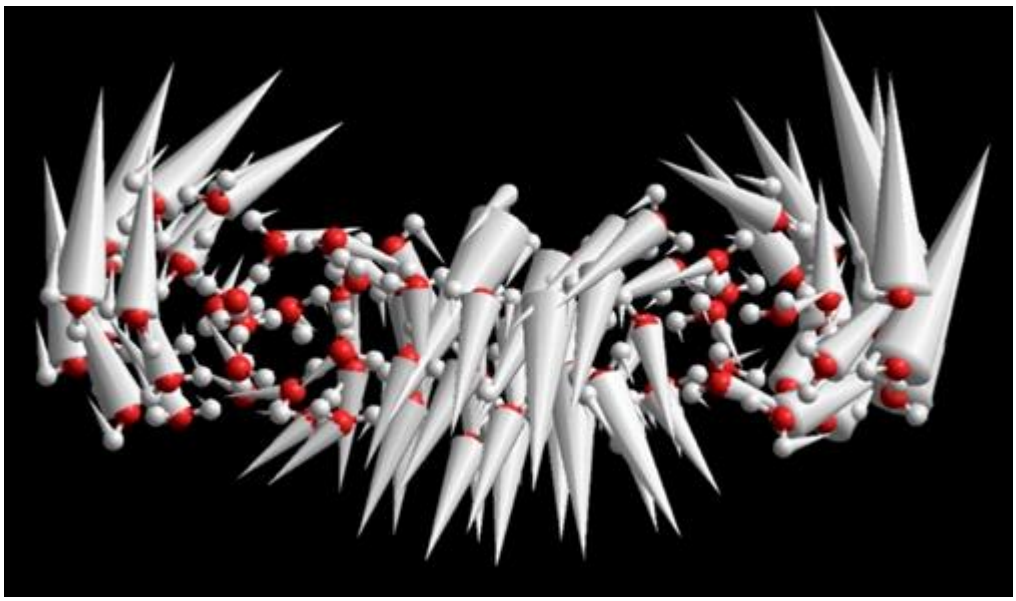

(**b**)

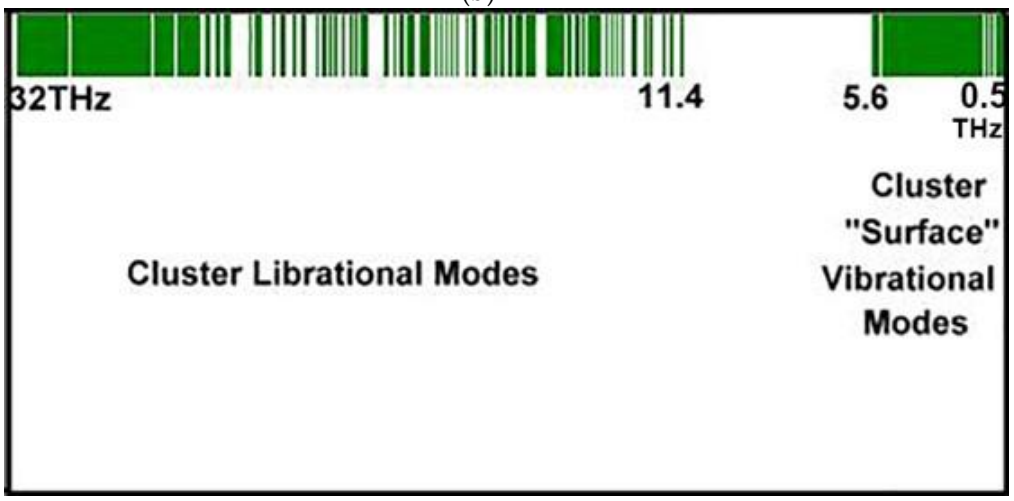

(**a**)

Figure 3. a. THz vibrational spectrum of a stable linear array of five pentagonal dodecahedral water nanoclusters calculated using the SCF-Xα-Scattered-Wave density- functional method (Reference 17). **b.** Lowest-frequency THz vibrational mode and relative vibrational amplitudes. Note the lower cutoff THz frequency compared to those in Figures 2e and f.

Figures 2 and 3 exhibit qualitative resemblance to Figure 1c,d but show a gradual decrease in the vibrational frequency cutoff as the cluster size increases. This trend aligns with experimental observations of THz radiation emission from water vapor nanoclusters [15], as depicted in Figure 4. The shift in THz emission peaks towards lower frequencies and intensities, corresponding to larger clusters, occurs with decreasing water vapor ejection pressure in the vacuum chamber where the radiation was measured. This observation suggests a decrease in THz emission cutoff frequencies and intensities as water nanoclusters of increasing sizes are ejected from ice-coated cosmic dust.

Preprints (www.preprints.org) | NOT PEER-REVIEWED | Posted: 16 November 2023 doi:10.20944/preprints202311.1084.v1

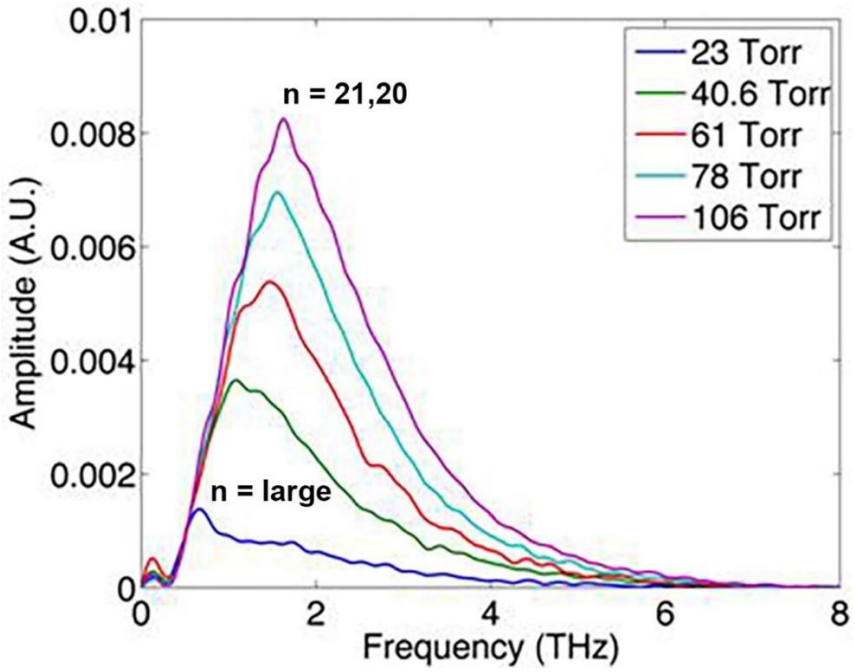

Figure 4. Frequency dependence for a range of pressures of the THz wave generation amplitudes (in arbitrary units) from water nanoclusters, $(H_2O)_nH^+$ and $(H_2O)_n$ produced from water vapor, described in Ref. 15. Maximum wave generation is associated with the "magic numbers," n = 20 and 21.

Common characteristics among all these water clusters include: (1) lowest unoccupied (LUMO) energy levels, akin to those in Figure 1a, corresponding to diffuse Rydberg cluster "surface" molecular-orbital wavefunctions depicted in Figure 1b as "S," "P," "D," and "F"-like orbitals and (2) bands of vibrational modes ranging from 0.5 to 6 THz (Figures 1–3) due to O-O-O "squashing" or "bending" and "twisting" motions between adjacent hydrogen bonds. The vectors in Figures 1–3 represent the directions and relative amplitudes of the lowest THz-frequency modes associated with the O-O-O "bending" (or "squashing") motions of the water-cluster "surface" oxygen atoms. Observations of surface O-O-O bending vibrations in this energy range have been performed under laboratory conditions [18]. Furthermore, ultraviolet excitation of an electron from the highest occupied molecular orbital (HOMO) to the lowest unoccupied molecular orbital (LUMO), as shown in Figure 1a, can place the electron into the Rydberg "S"-like cluster molecular orbital illustrated in Figure 1b. Occupancy of this orbital results in a bound state, even when an additional electron is introduced, leading to the formation of a "hydrated electron" [19]. In contrast, a water monomer or dimer exhibits virtually no electron affinity. Therefore, in space, particularly within dense interstellar clouds, a water nanocluster, $(H_2O)_{21}H^+$ or $H_3O^+(H_2O)_{20}$, ejected from amorphous water-ice-coated cosmic dust, is likely to capture an electron, leading to electrically neutral water nanoclusters, as shown in Figure 2.

3. Rydberg Dark Matter

Starlight energy can trigger electronic excitations from the $(H_2O)_{21}H^+$ HOMO (Figure. 1a) or the LUMO when a hydrated electron is captured. These excitations then shift to the more delocalized "P", "D", "F", and other higher water-cluster Rydberg orbitals shown in Figure 1b. These specific states exhibit minimal spatial overlap with lower-energy-filled states. Their longevity increases with increasing excitation energy and principal Rydberg quantum number. Thus, they become potential contenders for Rydberg Matter (RM) — a dilute phase of weakly bonded individual molecules in Rydberg excitation, which have extensive effective interactions [20]. RM is a *low-density* condensed phase of weakly interacting individual Rydberg-excited molecules over long-range intermolecular distances - approximately one micron for the $(H_2O)_{21}H^+$ Rydberg level, n = 80. RM is transparent at

Preprints (www.preprints.org) | NOT PEER-REVIEWED | Posted: 16 November 2023 doi:10.20944/preprints202311.1084.v1

visible, infrared, and microwave frequencies and thus, ignoring the observationally difficult emissive THz region (Figure 4), qualifies as dark matter.

Quantum entanglement of RM occurs because the diffuse nanocluster Rydberg molecular orbitals "overlap" even at relatively large distances. Pentagonal dodecahedral water nanoclusters, containing an excited or "hydrated" electron in the Rydberg "S" LUMO, resemble oversized hydrogen atoms (Figure 1b). When two such clusters are in close proximity, they can create an interlocking "Sσ-bonding" molecular orbital as depicted in Figure 5a, which accommodates two electrons with paired spins, mirroring a large hydrogen molecule. Elevating the electrons to the Rydberg "P" LUMO results in the formation of "Pσ" and "Pπ" molecular bonding orbitals, as shown in Figures 5b and 5c. However, it's uncommon for two water nanoclusters to come near each other in the interstellar regions because of their sparse distribution. At more significant distances between these clusters, the expansive molecular orbitals of their highest, most delocalized Rydberg states can overlap enough to allow quantum entanglement across vast spatial expanses.

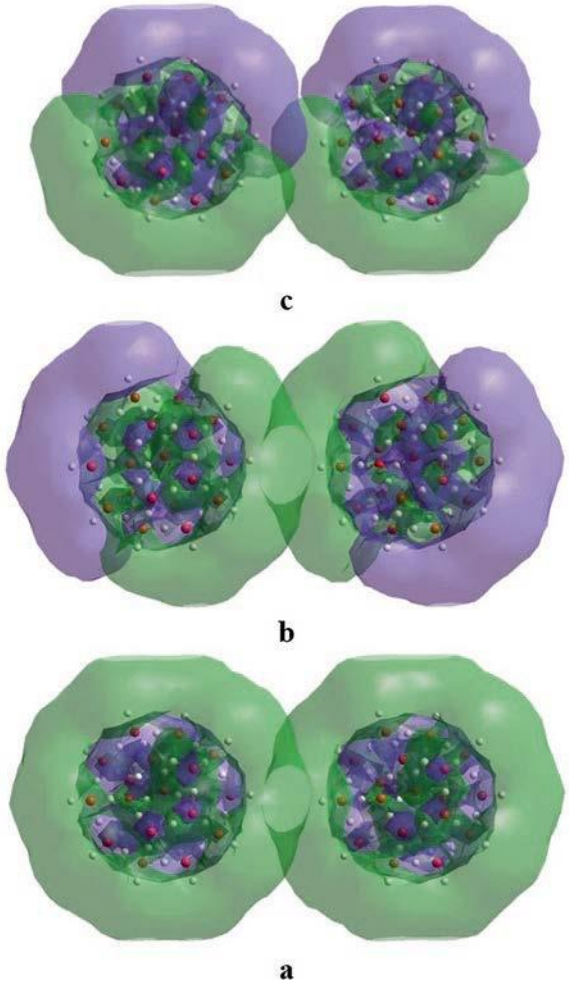

Figure 5. a. "Sigma-bond" molecular-orbital overlap of water-nanocluster Rydberg "S" LUMOs shown in Figure 1b. **b**. "Sigma-bond" molecular-orbital overlap of Rydberg "P" LUMOs. **c**. "Pi-bond" molecular-orbital overlap of Rydberg "P" LUMOs.

4. Observational Support

4.1. No Cosmic Dust – No Dark Matter

The Hubble Space Telescope has revealed a galaxy, NGC 1052-DF2, approximately 72 million light years from Earth, where one can literally see through other galaxies behind it [21] (Figure 6). It is an ultra-diffuse galaxy, almost as wide as the Milky Way, but contains only one 200th of the number of stars in the Milky Way. Furthermore, the galaxy contains at most only one four hundredth of the

Preprints (www.preprints.org) | NOT PEER-REVIEWED | Posted: 16 November 2023 doi:10.20944/preprints202311.1084.v1

amount of dark matter that astronomers expect from the standard dark matter theory. The ultra diffuseness of the galaxy also suggests a lack of cosmic dust characteristic of the Milky Way and most other galaxies. Thus, the proposal made in this paper that cosmic dust, coated with amorphous water-ice, produces water nanoclusters that constitute a type of baryonic dark matter is supported by the observation of galaxies such as NGC 1052-DF2, which are devoid of both cosmic dust and dark matter.

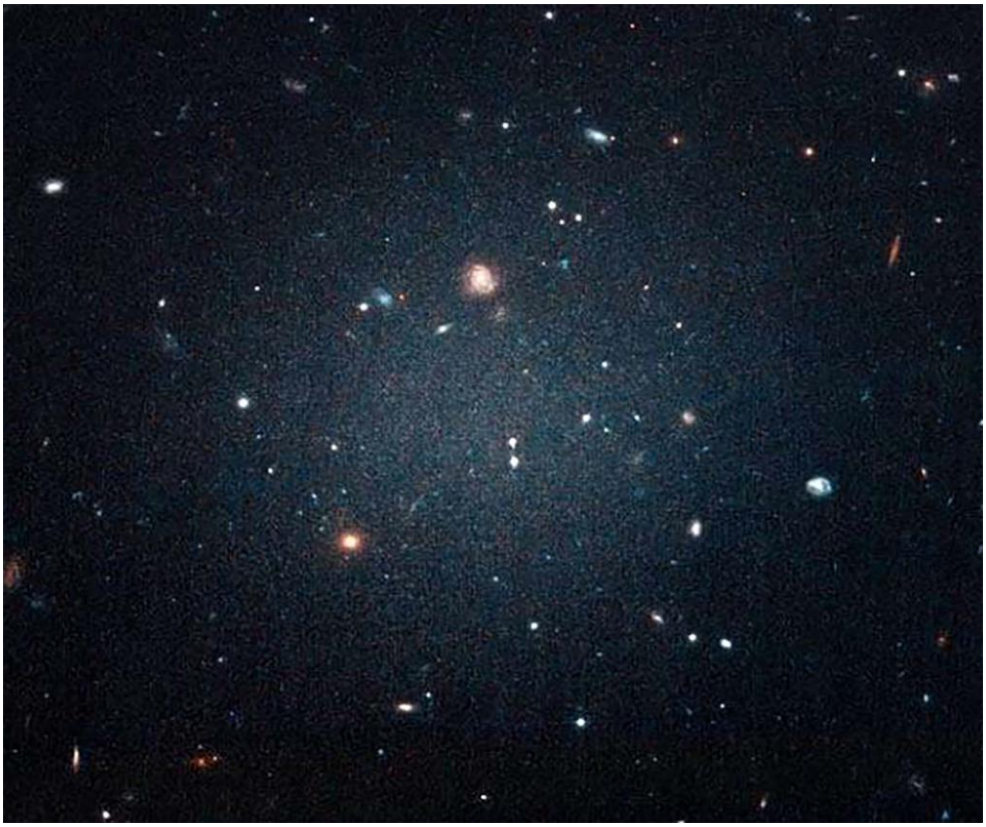

Figure 6. Galaxy NGC 1052-DF2. See Reference 21.

4.2. Cosmic Birefringence

Minami and Komatsu [22] have reported the extraction of cosmic birefringence data from the 2018 Planck Cosmic Microwave Background, which may possibly support "new physics" such as *quintessence*. A more recent publication [23] agrees with [22] and claims to be more precise than the previous paper, providing further evidence for physics beyond the standard model. The THz vibrations of cosmic water nanoclusters, ejected from amorphous water-ice-coated cosmic dust to interstellar space, produce the dipole-moment anisotropy necessary and sufficient for their birefringence property. Figure 7a illustrates the 1.8 THz vibrational mode of the cosmic water nanocluster $(H_2O)_{21}H$ which contains a hydrated electron. This mode has been shown to be key to the finely-tuned coupling of water nanoclusters with the prebiotic molecules necessary for RNA polymerization (see Section 11), and it is nearly equal in frequency to the cutoff value, $\nu_c \cong 1.7$ THz of vacuum fluctuations proposed to be responsible for dark energy (see Section 5). Dynamic Jahn-Teller symmetry breaking of the water-cluster dodecahedra produces the dipole moments along the nanocluster axes indicated in Figure 7a, computed by the SCF-Xα cluster density-functional method [17]. Such anisotropic dipole moments lead directly to the birefringence of water nanoclusters, as they do for the observed THz-induced birefringence of ordinary liquid water [24], which can be viewed as a dynamical random network of dodecahedral water clusters. Thus, the birefringence of cosmic water nanoclusters can explain the CMB birefringence from a condensed-matter point of view, instead of by unobserved elementary particles such as AXIONS [22,23].

Preprints (www.preprints.org) | NOT PEER-REVIEWED | Posted: 16 November 2023 doi:10.20944/preprints202311.1084.v1

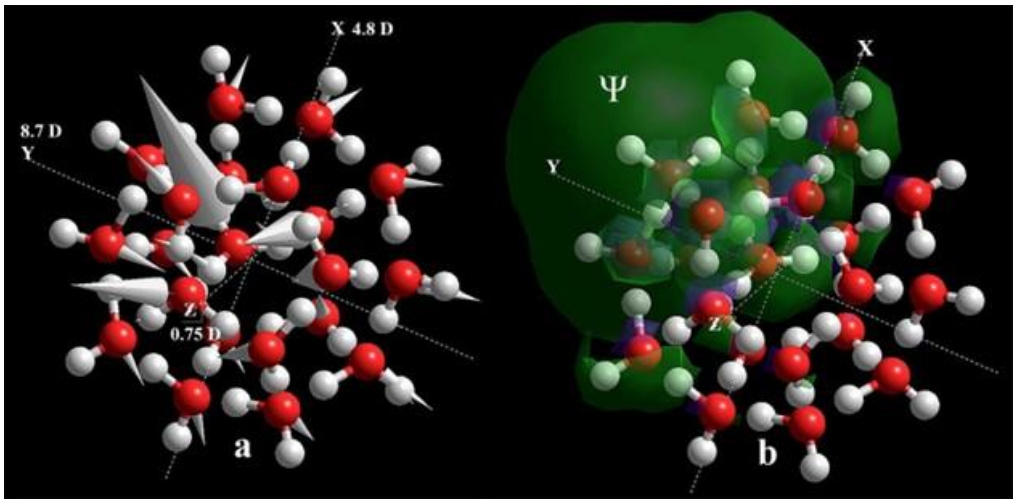

Figure 7. a. 1.8 THz vibrational mode of water nanocluster $(H_2O)_{21}H$ holding a hydrated electron. The component anisotropic dipole moments (in Debyes) along the nanocluster axes are shown. **b.** Wavefunction Ψ of the attached electron responsible for the anisotropic dipole moment.

4.3. The Bullet Cluster and Galactic Halos

Standard cosmology largely agrees that dark matter is not baryonic. One of the most compelling claims of evidence for the existence of dark matter is the gravitational lensing observations from the *Bullet Cluster*, which distinctly shows the separation between luminous matter and dark matter [25]. The protonated water nanoclusters, shown in Figure 1, are positively charged. However, it's suggested that these clusters might obtain a "hydrated" electron from space once they're ejected from cosmic dust that's ice-coated, transitioning into electrically neutral clusters like those in Figure 2. While it is generally accepted that dark matter is electrically neutral, recent discussions suggest that a small amount of charged dark matter might have played a role in cooling early universe baryons [26]. The dark matter properties of the Bullet Cluster might be linked to the electric charge of the ice-coated cosmic dust, which is believed to be the birthplace of cosmic water nanoclusters. Given that a significant portion of the Bullet Cluster's regular matter could be positively charged cosmic dust, this could amplify the ejection of protonated water nanoclusters, further highlighting the observed separation between luminous and dark matter. Even with existing uncertainties about galactic-scale electric fields, it is conceivable that these fields might promote the aggregation of cosmic water nanocluster RM around galaxy outskirts, possibly explaining the enigmatic galactic *dark matter halos*, akin to the dark matter observed in the Bullet Cluster. Despite uncertainties about electric fields on the galactic scale, it is possible that such fields over time can cause the expulsion of water-nanocluster RM into the outer dark-matter halo reaches of the galaxies, thereby explaining the recent observation [27] of a *direct interaction*, beyond gravitational, between dark matter and normal baryonic matter in galaxies. Such a direct interaction is consistent with the baryonic nature of cosmic water-nanocluster Rydberg dark matter. This creates spherical regions of relatively constant density within the dark matter halo, with dimensions that increase proportionately over time and finally reach those of the galactic stellar disc.

5. Dark Energy

5.1. The Cosmological Constant Problem

Quantum field theory proposes a vacuum energy density that exceeds the measured value by as much as 120 orders of magnitude. This discrepancy is rooted in the cosmological constant issue [1,28].

Preprints (www.preprints.org) | NOT PEER-REVIEWED | Posted: 16 November 2023 doi:10.20944/preprints202311.1084.v1

5.2. The Link Between Dark Energy and Vacuum Fluctuations

A proposition by Beck and Mackey [4] hints that equating the observed dark energy, driving the universe's accelerating expansion, to the cosmic vacuum energy density from theory implies a cut-off frequency for gravitationally active zero-point-energy vacuum fluctuations at around $\nu_c \cong 1.7$ THz. This suggests that only vacuum fluctuations with virtual photons below this frequency would be compatible with the relatively small observational data on dark energy.

5.3. Vacuum Fluctuations and Water Nanoclusters

Interestingly, this $\nu_c \cong 1.7$ THz frequency coincides approximately with the cutoff vibrational frequencies computed for specific water nanoclusters (Figures 1 and 2a). As these clusters grow, their frequencies reduce, as depicted in Figures 2b,c and 3. In contrast, other cosmic molecules, including hydrogen, water monomers, carbon buckyballs, and organic molecules, do not exhibit pure vibrational cut-off frequencies in this THz range.

5.4. Rydberg Matter as a Quintessence Scalar Field and the Dynamical Casimir Effect

Viewing cosmic water nanoclusters as a type of low-density Rydberg matter, they can potentially form a quintessence scalar field Q, characterized by an energy density, $\rho = \frac{1}{2}\dot{Q}^2 + V(Q)$ [29]. This field's properties might be influenced by the absorption of vacuum fluctuations' virtual photons with frequencies surpassing $\nu_c \cong 1.7$ THz, as detailed through the microscopic dynamical Casimir effect [5]. This absorption mechanism transforms virtual photons into real ones, as depicted in Figure 8, ensuring that only the lower frequency photons exhibit gravitational activity. The absorbed photons can decay, releasing THz radiation as displayed in Figure 4.

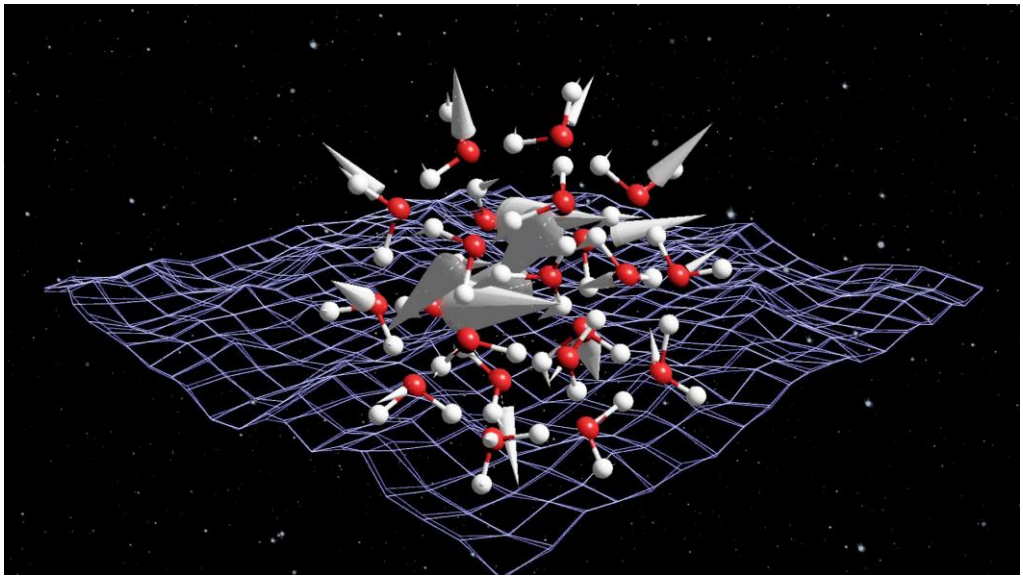

Figure 8. Dynamical Casimir absorption of vacuum fluctuation virtual photons by a cosmic water nanocluster, $\nu_c \cong 1.7$ THz vibrational mode.

5.5. Cancellation of the Vacuum Energy Catastrophe

To express the above scenario more formally, we traditionally regard the vacuum electromagnetic field (ignoring other fields) as a set of harmonic oscillators with normal-mode frequencies denoted by $\nu_{\boldsymbol{k}}$. By adding the zero-point energies of each of these oscillator modes, we arrive at the following energy density,

$$\rho_{vac} = \frac{E}{V} = \frac{1}{V}\sum_{\boldsymbol{k}}\frac{1}{2}h\nu_{\boldsymbol{k}} = \frac{4\pi h}{c^3}\int_0^\infty \nu^3\, d\nu, \quad (1)$$

Preprints (www.preprints.org) | NOT PEER-REVIEWED | Posted: 16 November 2023 doi:10.20944/preprints202311.1084.v1

where $\boldsymbol{k}$ represents the normal modes of the electromagnetic field which align with the boundary conditions set by quantization volume, V. As V tends towards infinity, it corresponds to the right-hand side. To circumvent the diverging integral in Equation (1), one can introduce a cap with the cut-off frequency ν_c determined by the Planck scale, as suggested [1]. Nonetheless, this introduces a vast vacuum energy, which still overshadows the cosmologically observed value by many orders of magnitude. Alternatively, if we deduct from Equation (1) the energy density,

$$\rho_c = \frac{4\pi h}{c^3}\int_{\nu_c}^{\infty} \nu^3 \, d\nu \quad (2)$$

associated with the capture by cosmic water nanoclusters of vacuum-energy virtual photons above the nanocluster cutoff vibrational frequency, ν_c, via the microscopic dynamical Casimir effect [5], the divergent integral in Equation (1) is predominantly negated. This results in the finite value presented in Equation (3), which can be associated with the dark energy density,

$$\frac{\boldsymbol{4\pi h}}{\boldsymbol{c^3}}\int_{\boldsymbol{0}}^{\boldsymbol{\nu_c}} \boldsymbol{\nu^3 \, d\nu} = \frac{\boldsymbol{\pi h \nu_c^4}}{\boldsymbol{c^3}} = \boldsymbol{\rho_{dark}}. \quad (3)$$

The vibrational kinetic energy of small nanoclusters, represented as ½$\dot{Q}^2$, is notably lower than their potential energy V(Q). This potential energy gets amplified to higher- THz-frequency "surface" vibrational modes (seen in Figures 1-3) when these nanoclusters capture vacuum photons, as illustrated in Figure 8. From this, we can infer that the quintessence scalar field pressure, given by P = ½$\dot{Q}^2$ – V(Q) [29], becomes more negative as ν_c increases, and thus with the increase of ρ_{dark}. Planck satellite observations highlight that dark energy currently accounts for 68.3% of the universe's total known energy. This corresponds to a dark energy density, ρ_{dark} = 3.64 GeV/m^3 . From this, the cutoff frequency, ν_c is determined to be 1.66 THz, which aligns with the frequencies observed in the smallest pentagonal dodecahedral water clusters (Figures 1d and 2a). It's also worth noting that as water-cluster size grows (as shown in Figures 2b,c and 3), ν_c *decreases*. Consequently, if larger water clusters were to be increasingly ejected with time from cosmic dust, it suggests that the density of dark energy would *decrease* over time as per Equation (3). This could imply a *slowing expansion* of the universe over cosmic time.

6. The Cosmic Microwave Background

6.1. The CMB Spectrum

The prevailing belief in standard inflationary cosmology [30] posits that the universe's cosmic microwave background (CMB) spectrum emerged approximately 380,000 years post-Big Bang. Given the THz vibrational attributes of water nanoclusters addressed earlier, is there another potential contributor to the CMB that aligns with its spectrum? Historically, some theories have proposed that CMB might be due to thermal effects caused by "dust." This dust was thought to manifest as either hollow, spherical shells with a high dielectric constant [31] or as conductive needle-like grains [32]. It was suggested that radiation emanating from galaxy-sized entities at a redshift, z ≅ 10, could be thermalized by a sparse concentration of such high-dielectric-constant dust. The large electric dipole moments of water nanoclusters (Figure 7a), in addition to their intense THz radiation emission [15], coincide with these criteria. Such water nanoclusters either form spherical "shells" of water-cluster O-H bonds (Figures 1&2) or needle-like aggregates (Figure 3). The amorphous layers of water-ice enveloping cosmic dust, from which these nanoclusters are derived, can be perceived as disordered nanoclusters possessing a high dielectric constant, and hence might also contribute. Astrophysical data revealed that the formation of early galaxies and reionization likely took place at redshifts, z = 8.6 and z = 9.6 [33,34]. This corresponds to approximately 600 million and 500 million years post-Big Bang, respectively. Additionally, more recent discoveries from the Hubble Space Telescope located a galaxy at z ≅ 11, equivalent to approximately 400 million years after the Big Bang [35]. Even larger-redshift galaxies are being claimed by the Webb telescope [36]. When considering a redshift of z ≅ 10,

Preprints (www.preprints.org) | NOT PEER-REVIEWED | Posted: 16 November 2023 doi:10.20944/preprints202311.1084.v1

the distinct THz vibrational spectra of the water clusters are redshifted into the frequency domain of the observed CMB spectrum, more specifically near the peak of the leftmost CMB component shown in Figure 9. This suggests the THz emission from water nanoclusters originating around z ≅ 10, where the temperature is approximately 30K (thus allowing the existence of such clusters), might compete with the Big Bang CMB contribution originating from the earlier "recombination" phase at z ≅ 1100, where temperatures were around 4000K.

6.2. The CIRB Spectrum

The Cosmic Infrared Background (CIRB) is the light radiated from stars within innumerable dim galaxies. When one accounts for emissions from our solar system and the Milky Way, the CIRB spectrum shown in Figure 9 persists. The near-infrared region with wavelengths of approximately 2-3 microns, corresponds to starlight that has redshifted in the infrared region. However, some starlight is also assumed to be absorbed by cosmic dust, which then emits it again in the far-infrared region, approximately 100 μm. However, it is proposed in this paper that cosmic dust, enveloped by amorphous water-ice, is composed of and ejects into space water nanoclusters, as depicted in Figures 1d and 2a. The water clusters present at z = 10 not only emit THz radiation that is redshifted to the leftmost CMB peak in Figure 9, but also, since they should exist in our Milky Way galaxy, contribute to the foreground radiation between approximately one and six THz in Figure 9. Indeed, the peak intensity shown around 1.5-1.7 THz may be associated with the dodecahedral water-nanocluster vibrational cutoff frequencies indicated in Figures 1d and 2a. This is the same maximum emission frequency of water clusters produced from water vapor in a laboratory vacuum, as shown in Figure 4 [15].

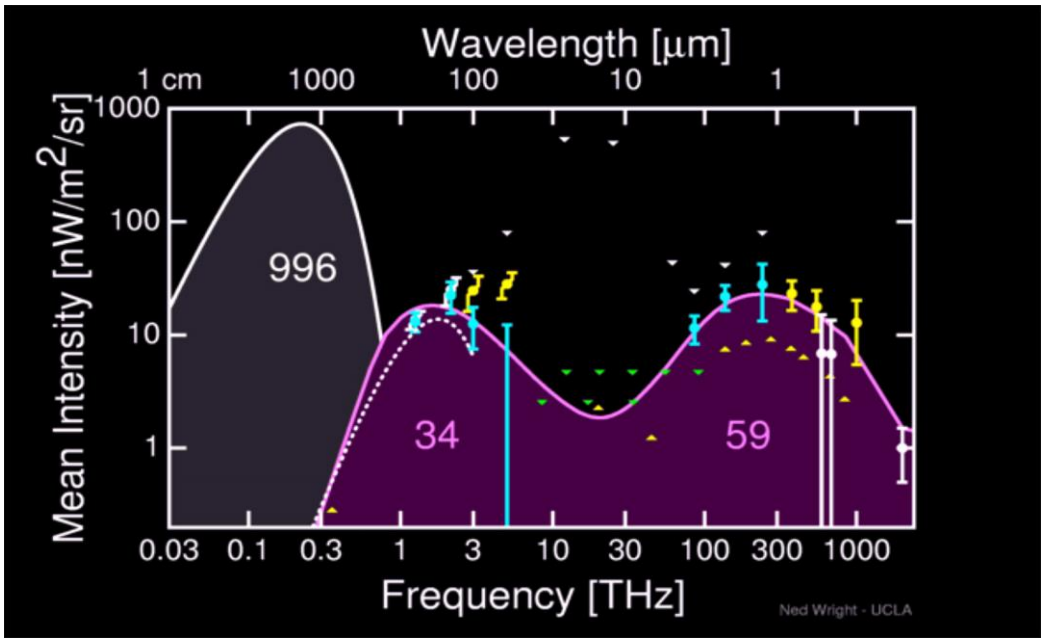

Figure 9. The Cosmic Infrared Background (CIRB) compiled by Ned Wright of UCLA.

The data points correspond to a wide variety of observations.

The laboratory measurements displayed in Figure 4 demonstrate that when water nanoclusters emit THz radiation and are subjected to different ejection pressures in a vacuum chamber, the emission peaks change. Specifically, as the pressure decreased, both the frequency and intensity of the emission decreased. This corresponds to an increase in the size of the water clusters, as illustrated in Figures 2 and 3. The strongest emission, at 1.7 THz, is linked to water clusters of “magic numbers” n = 21 and 20 (Figure 4). The peaks that reduce in frequency and intensity down to roughly 0.5 THz can be attributed to larger clusters, as shown in Figures 2b,c and 3a. Notably, the smaller the water nanocluster, the higher the frequency of its emitted radiation, peaking near 1.7 THz. Drawing a

Preprints (www.preprints.org) | NOT PEER-REVIEWED | Posted: 16 November 2023 doi:10.20944/preprints202311.1084.v1

comparison with cosmic scenarios, if we consider the radiation from water nanoclusters ejected from water-ice-covered cosmic dust at around z ≅ 10, the redshifted emission from smaller versus larger clusters qualitatively resembles the CMB power spectrum. Further insights from the laboratory data [15] (Figure. 4), when connected with the ejection of water nanoclusters from cosmic dust, hint at a "pressure wave" originating around z ≅ 10, which is about 500 million years post the Big Bang. This bears similarity to the CMB acoustic wave from the "recombination" period at z ≅ 1100, approximately 380 thousand years after the Big Bang. In simpler terms, if we consider the observed CMB power spectrum to be even partly due to the redshifted THz radiation from cosmic water nanoclusters, it suggests a possible "turning point" for a *cyclic* expansion of our universe (see Section 9), in contrast to the inflationary Big Bang scenario originating from a singular quantum point. An interesting fact to ponder is that z ≅ 10, or about 500 million years after the alleged Big Bang, aligns with the speculated period of the earliest (Population III) star formation. Most of these theorized stars would have short lifespans and quickly become supernovae which explode to cosmic dust that ejects water nanoclusters, which then act as coolant for rapid star creation (see Section 7), offering an explanation of the growing Webb telescope evidence for early galaxy formation [36].

6.3. CMB Polarization: E- and B-Modes

Recent Planck satellite observations ascribed to foreground cosmic dust polarization in our galaxy have revealed that the power of the E-mode polarization is approximately twice that of the B-mode [37], although they are expected to be equal. Understanding this fact may be key to experiments looking for *primordial* B-modes leftover by inflationary gravitational waves, such as the infamous Antarctic BICEP2 experiments of 2014, which were dominated by foreground dust polarization after initial claims of primordial B-modes as possible support for cosmic inflation [38]. The E/B-mode polarization ratio can be explained not by the dust alone, but by the polarization of the water nanoclusters that comprise and are ejected from the amorphous water-ice enveloping the dust particles. This is due to the power of the three water-cluster H_g "squashing" vibrational modes compared to the power of the two H_u "twisting" modes represented in Figure 10, where the power is proportional to the squares of their amplitudes. They vibrate and twist over a 1-6 THz frequency range, possibly contributing redshifted radiation to the CMB and CMBIR.

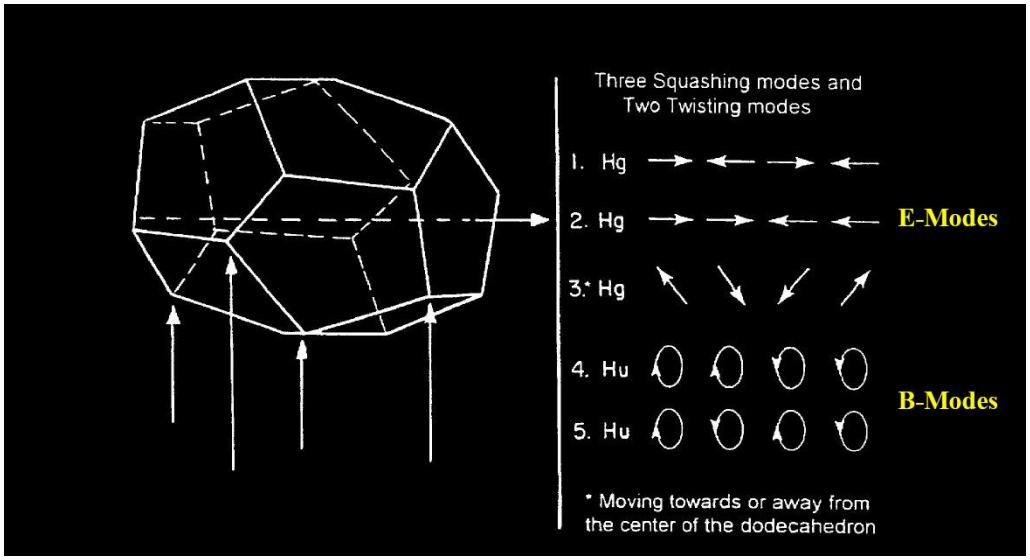

Figure 10. E- and B- vibrational modes of a pentagonal dodecahedral water nanocluster.

7. Cosmic Water Nanoclusters and Early Star Formation

Water vapor has been identified as a cooling agent in the process of star formation [8]. A remarkable finding revealed a vast water reservoir within a high-red-shift (z ≅ 4) quasar, which had a water vapor mass surpassing 140 trillion times the combined water of the Earth's oceans and was

 doi:10.20944/preprints202311.1084.v1

100,000 times more massive than the sun [10]. This, coupled with the suggestion [11] that water vapor might have been prevalent roughly a billion years post-Big Bang, leads to the hypothesis that there might have been a considerable presence of water nanoclusters approximately 500 million years after the Big Bang or at redshift z ≅ 10. The rapid rate of star formation from dense gas clouds observed at z ≅ 6.4, which is approximately 850 million years after the Big Bang [39], might be better understood considering the potential role of these water nanoclusters in aiding the cooling effects of the cloud's water vapor. Research on the infrared absorption of water nanoclusters, both in a controlled environment and within Earth's atmosphere, has shown that these clusters possess remarkable heat storage capabilities [12,40]. This property is attributed primarily to the *librational modes* of these nanoclusters, especially those around the frequency of 32 THz (1060 cm-1), as depicted in Figures 1 and 2. Consequently, the cooling process in star-forming gas clouds could potentially be driven by the emission of photons related to the mainly-oxygen vibrations on the cluster surface, falling within the 1–6 THz spectrum, as illustrated in Figures 1 and 2. Intriguingly, these photons might influence the CMB. In other words, if we accept the idea that THz radiation from spaceborne water nanoclusters around z ≅ 10 plays a role in the CMB spectrum, then the CMB might also offer clues about the early stages of star formation.

8. Hubble Tension

The current model possibly explains the *Hubble tension*, where the Hubble constant value derived from observing supernovae suggests a faster expanding universe compared to values from CMB readings immediately after the Big Bang. It posits that cosmic dust enveloped by amorphous water-ice, which ejects water nanoclusters linked to dark energy and the acceleration of the universe, stems from stellar evolution. Given that the birth of the initial stars occurred after the reionization phase that succeeded the hydrogen formation recombination phase starting approximately 380,000 years post-Big Bang, substantial cosmic dust and, subsequently, cosmic water nanoclusters would not form until significantly later. This theory is bolstered by a recent sighting of the earliest cosmic dust 200 million years after the emergence of the first stars [41]. Over the universe's 13.8-billion-year expansion, cosmic dust volumes rose with more stars and galaxies emerging, culminating in today's sufficient dust and ejected water-nanocluster Rydberg matter to justify the recent value of the Hubble constant from supernovae observations.

9. Cosmic Water Nanoclusters and a Cyclic Universe

Inflationary cosmology suggests that in an expanding universe, dark matter's density diminishes more rapidly than dark energy's. This implies that dark energy will eventually take precedence, leading to a future where all cosmic matter is progressively dispersed by this expansion – a scenario often termed the "big rip." On the other hand, if we consider thar cosmic water nanoclusters, which emerge from the water-ice-encrusted cosmic dust as Rydberg matter, are analogous to a time-varying quintessence scalar field, as discussed in Section 5.4, our model introduces a potential cyclical relationship between dark matter and dark energy in the cosmos:

(1) As the universe expands and stars produce heavier elements, more amorphous water-ice-coated cosmic dust will arise from an increased number of supernovae. This dust increasingly releases larger water clusters owing to the expanding space and lower pressure, as shown in Figure 4. Figures 1-3 indicate that larger water clusters will have a decreasing vibrational cutoff frequency, ν_c.

(2) Over time, as larger water clusters become more common, their vibrational cutoff frequency will tend towards ν_c ≅ 0.5 THz (see Figures 3 and 4) and likely even lower. This leads to a much-reduced dark energy density, ρ_{dark} (see Equation 3), nearing zero, which implies a slowing expansion of the universe.

(3) Eventually, the gravitational pull from the remaining cosmic matter, resulting from fewer supernovae, dominates. The universe will cease its expansion, start contracting, and revert to a possible state such as 500 million years post Big Bang, where it is roughly 10% of its current size.

Preprints (www.preprints.org) | NOT PEER-REVIEWED | Posted: 16 November 2023 doi:10.20944/preprints202311.1084.v1

(4) When this happens, the pressure from the anticipated water-nanocluster vapor around $z \cong 10$ will rise. As per Figure 4, smaller water nanoclusters, particularly with magic numbers n = 21,20 and higher ν_c (seen in Figures. 1d and 2a), will become more prevalent. These clusters will serve as cooling agents for star formation (Section 7), leading once again to supernovae and the production of cosmic dust that produces water nanoclusters.

(5) This scenario provides a potential "turning point" for *non-inflationary re-expansion*, though further collapse and water vapor decomposition are possible to offer hydrogen for star development. These cycles, influenced by supernovae patterns, span billions of years, although the exact durations are uncertain. This *cyclic universe* model aligns qualitatively with others [42,43] and challenges the multiverse concept, which is a derivative of inflation theory.

(6) This theoretical model does not contradict the second law of thermodynamics because of the cyclic formation of low-entropy water nanoclusters. It also suggests that our current period in the universe's expansion might be the most conducive for life as we understand it, a topic expanded upon in the following sections on astrobiology, the RNA World [7], and the origin of life in the universe.

10. Astrobiology

Determining the origin of Earth's water is crucial for comprehending the beginnings of habitats conducive to life and gauging the frequency of such habitats in the cosmos. A recent study suggested that if the formation of our solar system is a common occurrence, plentiful interstellar water-ice would be accessible to all emerging planetary systems [44]. This amorphous ice envelopes cosmic dust and ejects to interstellar space quintessential water nanoclusters, which constitute a form of Rydberg baryonic dark matter and absorb vacuum energy, accounting for the magnitude of dark energy, as described in the preceding sections.

Over the past five decades, the identification of *organic* molecules, including those with potential prebiotic roles, in interstellar spaces, dust clouds, comets, and meteorites has been noteworthy [45–47]. While much attention has been paid to the role of cosmic carbon compounds in the potential existence of life across the cosmos, *water* remains fundamental to the makeup and function of carbon-based life forms. Considering the human body, which is about 70% water and the human brain, which is 75% water, the importance of water in biology is clear, particularly in the creation of RNA, DNA, and proteins. A significant portion of this water binds to proteins, RNA, and DNA in the form of nanoclusters known as "structured water" [6]. Without such nanostructured water, proteins fail to fold correctly, potentially resulting in degenerative diseases such as Parkinson's, Alzheimer's, and cataracts. Structured water is crucial for RNA and DNA replication. The interaction between water nanoclusters and organic molecules in astrobiology can be explored through first-principles quantum chemistry calculations, specifically the SCF-Xα-Scattered-Wave density-functional method [17]. Originally, this approach was used for protein research [48–50]. Figure 11 shows the resultant molecular structures and their primary THz-frequency vibrational modes when a pentagonal dodecahedral water nanocluster interacts with *methane*, *anthracene*, and *valine*. Notably, each has been discovered in cosmic entities such as interstellar spaces, dust clouds, comets, and meteorites [45–47]. In all instances, there's a 1.8 THz water-cluster oxygen motion link to carbon atomic movements, depicted by the vectors in Figure 11. In anthracene and valine, the presence of C-C bonds means the 1.8 THz carbon movements induced by the water cluster manifest as bond "bending" modes. For valine, there's also a connection between the 1.8 THz vibrational mode of the water cluster and the motion of the nitrogen atom (Figure 11f). Valine, an α-amino acid, contributes to protein biosynthesis through a polymerization process starting with nitrogen and ending with carbon. The central idea is that water nanoclusters and prebiotic molecules brought to Earth by cosmic debris could have been a catalyst for life both on our planet and on exoplanets situated within the habitable zones of distant star systems. This process necessitates the formation of the first self-replicating RNA, laying the groundwork for DNA and protein synthesis from amino acids.

Preprints (www.preprints.org) | NOT PEER-REVIEWED | Posted: 16 November 2023 doi:10.20944/preprints202311.1084.v1

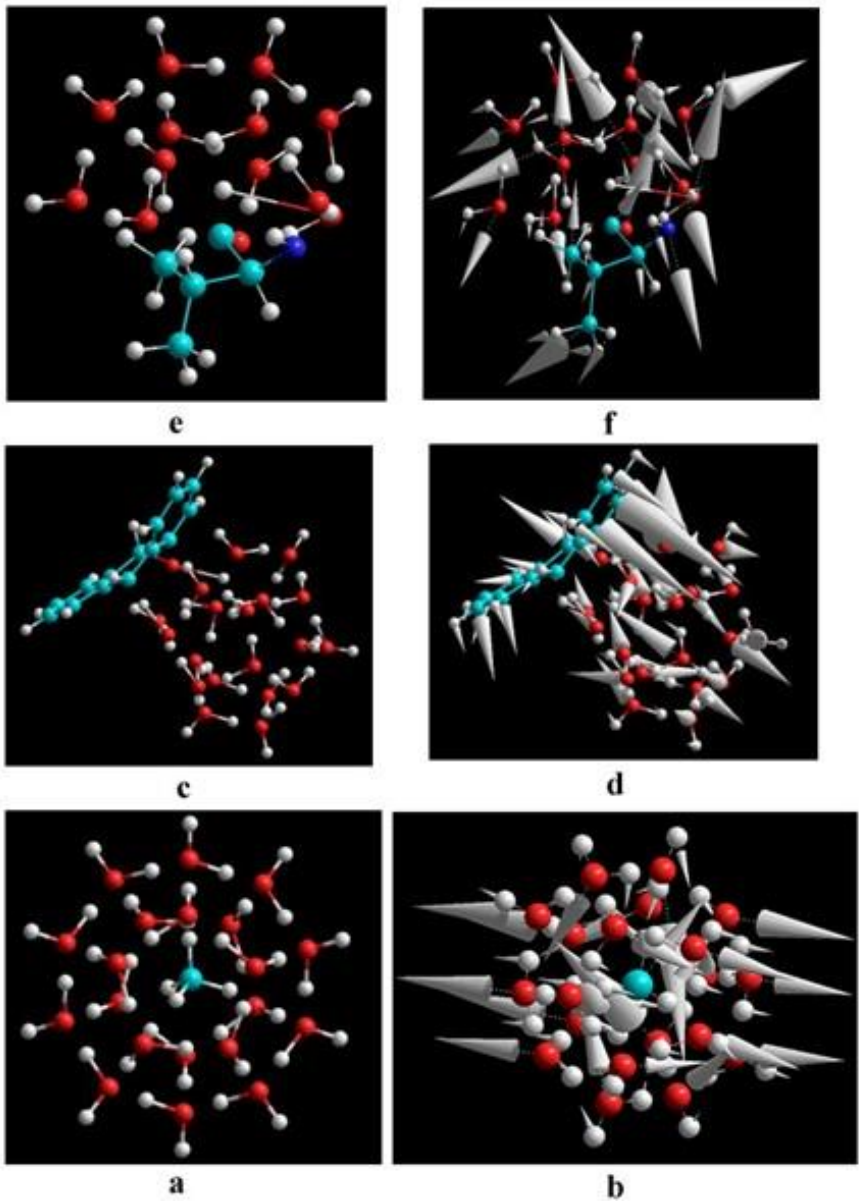

Figure 11. a. Pentagonal dodecahedral $CH_4(H_2O)_{20}$ methane clathrate. **b.** 1.8 THz vibrational mode. **c.** $(H_2O)_{20}$ cluster interacting with anthracene. **d.** The vibrational coupling of the $(H_2O)_{20}$ 1.8 THz vibrational mode to a THZ "bending" mode of anthracene. **e.** Hemispherical pentagonal dodecahedral water nanocluster enveloping a valine amino acid residue. **f.** Vibrational coupling of the water clathrate 1.8 THz vibrational mode to the valine amino acid "bending" mode.

11. The RNA World

Much evidence supports the *RNA World* hypothesis, suggesting that life on Earth, and possibly elsewhere in the cosmos, begins with RNA before the emergence of DNA and proteins [7,51]. This leads to a pivotal question: How did the initial self-replicating RNA molecules, such as the one illustrated in Figure 12, chemically evolve from a mix of pre-existing organic compounds, nucleosides, and phosphates? Although the formation of extensive RNA chains in water has been observed without a conclusive explanation [52], this discussion introduces the idea that water nanoclusters could serve as catalysts for the inception of RNA in early life creation, enhancing the probability of RNA-based worlds wherever water exists in the habitable zones of developed solar systems. In simpler terms, the chemical process that transforms the prebiotic components illustrated in Figure 12 into an RNA chain composed of nucleobases, *guanine*, *adenine*, *uracil*, and *cytosine*

Preprints (www.preprints.org) | NOT PEER-REVIEWED | Posted: 16 November 2023 doi:10.20944/preprints202311.1084.v1

involves the removal and reintegration of 11 water molecules. This process is known as the *dehydration-condensation* reaction [53]. Water pentamers [54], as shown in Figure 12, play a crucial role in the hydration and stabilization of biomolecules [55]. These structures often encase amino acids (Figure 11e,f), emphasizing water's geometric affinities with these compounds. Research on unique water states, such as supercooled water and amorphous ice, has revealed *cyclic* water configurations [56,57]. This discovery suggests the potential transportation of these structures to Earth-like planets through cosmic dust and meteorites. At the opposite extreme temperatures and pressures of hydrothermal ocean vents arising from planetary volcanic activity, expelled water can be in the *supercritical* phase, where the structure is neither liquid nor vapor but instead isolated water nanoclusters [58]. Therefore, at both temperature and pressure extremes, water pentamers interacting with prebiotic molecules could nucleate additional water molecules - eleven in the Figure 12 example - to form the more stable pentagonal dodecahedral cluster $(H_2O)_{21}H^+$, which could then provide via its THz vibrations (Figure 1c,d) the 11 water molecules necessary to yield the RNA sequence shown in Figure 12. Essentially, water nanoclusters, whether from space or deep-sea vents, may have set the stage for RNA synthesis. In other words, water nanoclusters delivered by cosmic dust and meteorites, or hydrothermally to planet Earth and habitable exoplanets could have provided a catalytic pathway for the dehydration-condensation mechanism of RNA polymerization.

The mechanism by which the $(H_2O)_{21}H^+$ cluster releases water molecules to aid the growth of RNA chains warrants further exploration. As described in Section 2, this protonated water cluster readily takes up an extra electron into the LUMO (Figure. 1a) – a hydrated electron [19] – as shown in Figure. 7. The proximity of the resulting electrically neutral $(H_2O)_{21}H$ cluster occupied LUMO "S" orbital to the lowest unoccupied, nearly degenerate cluster "P_x,P_y,P_z" orbitals (Figure 1a,b) suggests the possible coupling between the hydrated electron and the pentagonal dodecahedral cluster THz-frequency "squashing" and "twisting" modes shown in Figure 13a via the dynamic Jahn-Teller (JT) effect [59].

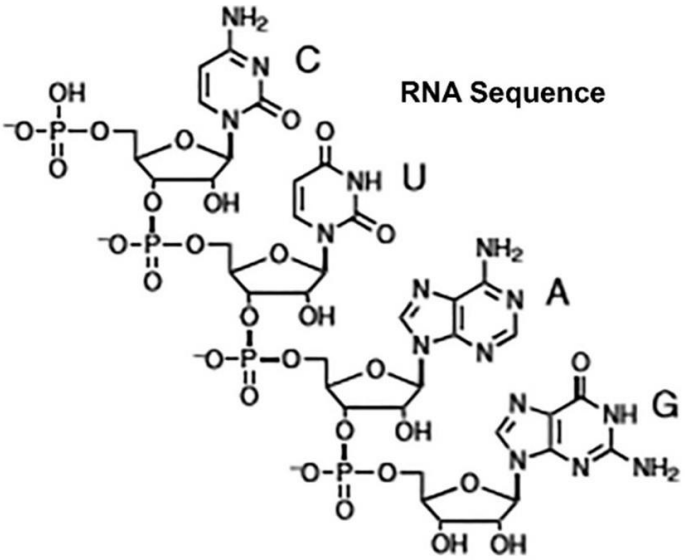

Preprints (www.preprints.org) | NOT PEER-REVIEWED | Posted: 16 November 2023 doi:10.20944/preprints202311.1084.v1

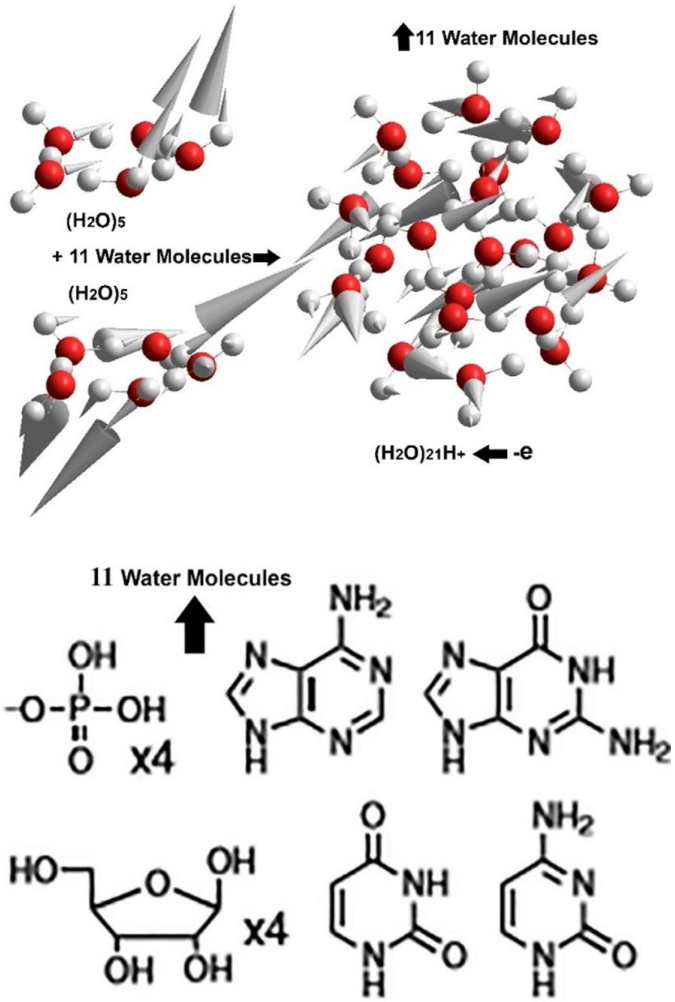

Figure 12. Dehydration-condensation exchange of eleven water molecules between prebiotic nucleosides and phosphates to form an RNA sequence of four polymerized nucleobases, *guanine*, *adenine*, *uracil*, and *cytosine* via a water nanocluster catalytic pathway.

JT coupling in $(H_2O)_{21}H$ leads to the prescribed symmetry breaking of a pentagonal dodecahedral water cluster (Figure 13a) along the THz-frequency vibrational mode coordinates Q_s, lowering the cluster potential energy from A to the equivalent minima A′ shown in Figure 13b. Because of the large JT-induced vibrational displacements (large Q_s) of water-cluster surface oxygen atoms, the energy barrier for expulsion of water oxygen or OH groups and their addition to reactive nucleotides is lowered from $E_{barrier}$ to $E'_{barrier}$.

Preprints (www.preprints.org) | NOT PEER-REVIEWED | Posted: 16 November 2023 doi:10.20944/preprints202311.1084.v1

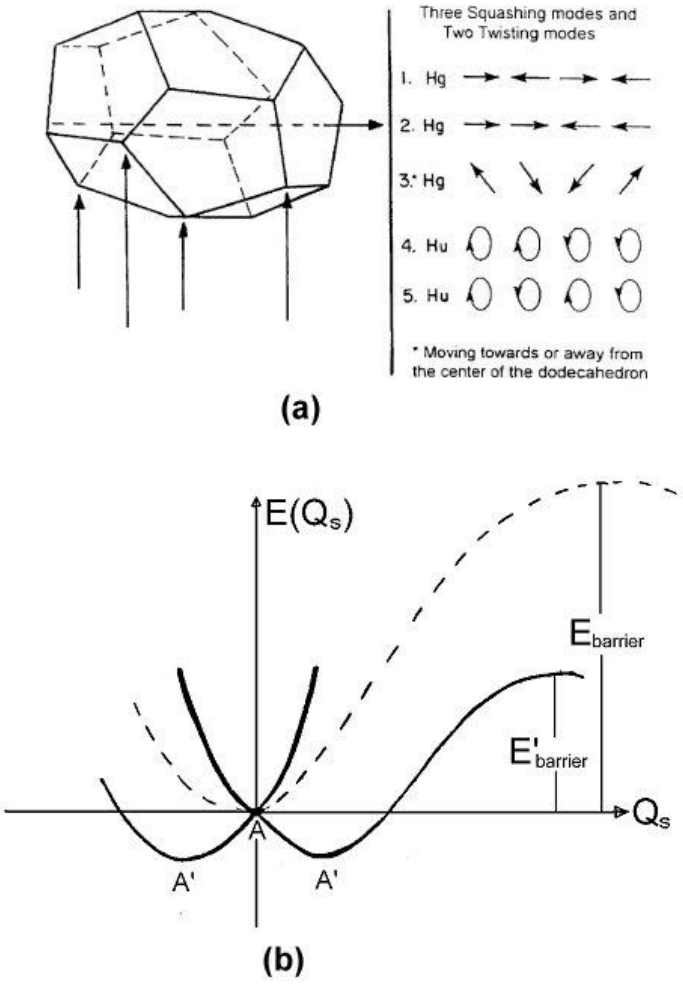

Figure 13. a. "Squashing" and "twisting" vibrational modes of a dodecahedral water cluster, where Hg and Hu designate the key irreducible representations of the icosahedral point group corresponding to these modes. Also see Figure 10**. b.** Schematic representation of the double potential energy wells for a Jahn-Teller distorted pentagonal dodecahedral water nanocluster and the resulting reduction of the energy barrier for the catalytic reaction of the cluster along the reaction path defined by the normal mode coordinates Q_s.

12. The Genesis of RNA-Based Protocells

Research into potential origins of life on our planet has yielded the construction of rudimentary protocell models in laboratories [60–63]. Notably, simple fatty-acid vesicles, which house snippets of RNA, were formed. These fatty acids are molecules characterized by their *amphiphilic* nature, meaning that they consist of both polar and nonpolar groups. Prebiotic conditions, akin to Earth's initial hydrothermal environments and extraterrestrial influxes, have often resulted in the presence of these fatty acids in experimental settings [64]. Diving into the intricate molecular behaviors, quantum- chemical assessments, particularly using the SCF-Xα Scattered-Wave density-functional method [17], have shown the natural fatty acid, glycerol monolaurate (GML-monolaurin), draws in water molecules, leading to the formation of a stable complex involving the water and the fatty acid, visualized in Figure. 14a. These insights indicate two things: first, the polar section of the fatty acid

Preprints (www.preprints.org) | NOT PEER-REVIEWED | Posted: 16 November 2023 doi:10.20944/preprints202311.1084.v1

contributes an electron to the water cluster, as shown in Figure 14a. Second, there's a vibrational resonance between the fatty acid chains and the water nanocluster, portrayed in Figure 14b. Such quantum interactions potentially bolster the chemical reactivity of fatty acids with early organic compounds, thereby facilitating RNA synthesis, as illustrated in Figure 12. As these interactions were prevalent in early Earth's conditions, the fatty acid molecules likely grouped around the emerging RNA chains, as shown in Figure 14c. This arrangement suggests an initial *reverse micelle* structure, a basic self-forming fatty-acid vesicle known to hold RNA fragments. This nascent paradigm offers a glimpse into the inception of cellular existence on Earth and potentially other life-bearing exoplanets. It also suggests the emergence of primeval RNA viruses [65] and has contemporary biomedical relevance [66].

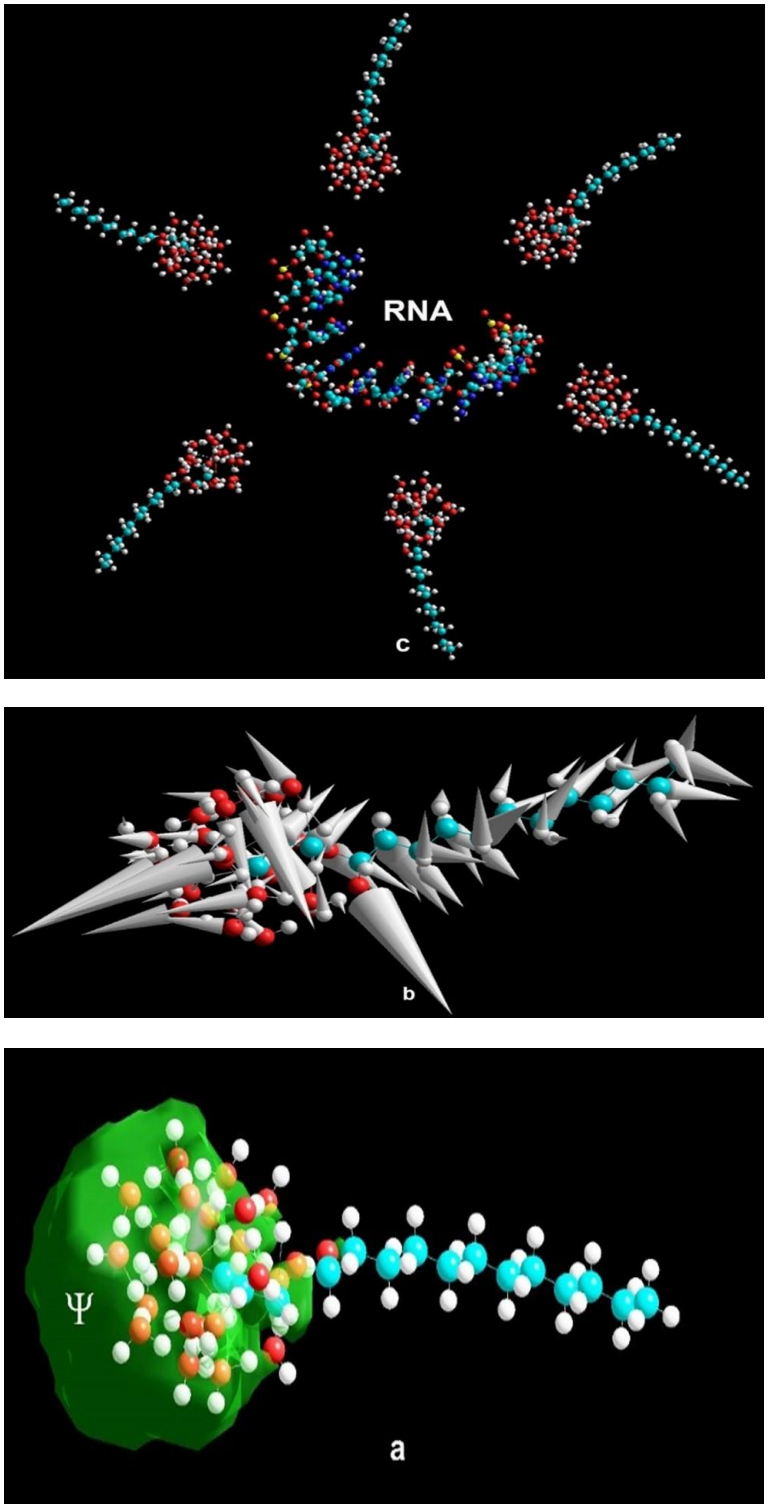

 doi:10.20944/preprints202311.1084.v1

Figure 14. a. Water nanocluster attached to the polar end of the naturally occurring fatty acid *glycerol monolaurate* (*"GML/monolaurin"*) $C_{15}H_{30}O_4$, which donates an electron to the water-cluster LUMO represented by the computed molecular-orbital wavefunction Ψ. **b.** The 1.8 THz vibrational mode of the combined water-nanocluster-GML molecule. Such quantum-mechanical coupling of fatty acids to water nanoclusters can promote their chemical reactivity with the prebiotic organic molecules and phosphates, leading to RNA polymerization by the steps shown in Figure 12. **c.** The aggregation of water-nanocluster-GML molecules around an RNA segment, forming a primitive reverse micelle.

13. Fundamental Frequency Findings

My quantum chemical research has revealed that water-nanocluster vibrational modes around 1.8 THz play a pivotal role in interacting with and energizing prebiotic molecules. Intriguingly, this frequency is close to the dark-energy cutoff frequency, $\nu_c \cong 1.7$ THz. As referenced in Section 5.5 and using Equation (3), this frequency signifies the current dark energy density caused by vacuum fluctuations. This aligns with the observed cosmological constant in the universe's ongoing expansion. Furthermore, these findings support the notion that water nanoclusters with "magic-numbers" of n = 21 and 20 water molecules, as depicted in Figures 1d and 2a, are the predominant forms generated by amorphous icy cosmic dust. In exploring the roles that water nanoclusters play in cosmology and astrobiology, there's a significant focus on pentagonal dodecahedral clusters. These "magic-number" nanoclusters' stability can be attributed to the water molecule's bond angle being closely aligned with that of a standard pentagon. As a result, there's only minimal deformation in the water molecule's hydrogen bonds. However, this doesn't entirely exclude the potential of other water nanocluster shapes being ejected from cosmic dust. For instance, the cutoff vibrational frequency of an icosahedral "water buckyball" is just slightly more than its pentagonal dodecahedral counterpart. Only minor changes in frequency result when deforming the latter dodecahedron. As cluster size grows (as exemplified in Figures 2b,c, and 3), both the cutoff frequency, ν_c and the dark energy density described by Equation (3) will be lesser than current measurements. Delving into the concepts of cyclic cosmology from Section 9 and the principles of astrobiology from Section 10, it's evident that as the universe expands, larger water nanoclusters, formed from icy cosmic dust, will emerge. However, these enlarged clusters will not be as efficient in interacting with prebiotic molecules. This suggests a decrease in the likelihood of life forming as cosmic time progresses. Essentially, our current period in the universe's expansion might be the most conducive for the emergence of life as we understand it. Thus, water nanoclusters, like those highlighted in Figures 1d and 2a, which originate on cosmic dust, could very well serve as life's catalysts, triggering the formation of RNA.

14. Discussion

While this study ventures beyond the prevalent inflationary cosmology and multiverse theory landscape, it's not the sole divergent view. Various cyclic-universe theories have gained attention and have offered critiques of the multiverse notion [42,43]. This paper presents a consolidated approach that bridges cyclic cosmology with the genesis of life, using quantum astrochemistry as its foundation, while integrating pertinent astrophysical insights. The notion that water nanoclusters could represent a type of invisible Rydberg baryonic dark matter does not eliminate the possibility of nonbaryonic dark-matter particles, such as WIMPS and AXIONS, although their observational evidence remains elusive [67]. As for dark energy, this study suggests that water nanoclusters could constitute a *quintessence* scalar field permeating space and absorbing the excess vacuum energy density, as quantified in Equations (1-3), during this cosmic era. This view is compatible with the proposed dark matter "web" pervading the universe [68]. Additionally, the findings of a neutral hydrogen bridge between the Andromeda (M31) and Triangulum (M33) galaxies [69] suggest that these water nanoclusters are dispersed similarly, acting as Rydberg dark matter. The remarkable alignment of the THz vibrational frequencies of these nanoclusters with the vacuum energy THz frequency, which parallels the dark-energy density in line with the cosmological data, might merely be coincidental. However, considering a shared origin for both dark matter and dark energy outside conventional particle physics—a field yet to definitively pinpoint the sources of these phenomena—

is enticing. Conceptually, these nanoclusters may represent baryonic nanoparticles that disrupt the otherwise uniform vacuum of space. Notably, their masses are similar to those estimated for WIMPS. No other known baryonic entities, including hydrogen and organic molecules, share these attributes and simultaneously qualify as dark matter. While fullerene buckyballs in nebulae [70] are also not candidates, cosmic entities like planets, moons, and asteroids that are covered by water-ice in various celestial environments must be considered potential water-nanocluster sources. For example, water clusters have recently been detected in the hydrothermal plume of Enceladus – a moon of Saturn [71]. In conclusion, when considering the quantum-chemical dynamics between cosmic water nanoclusters and organic molecules, and the potential for life on Earth and exoplanets, this perspective aligns with the *anthropic principle* [28]. It posits that our universe, viewed as a unified dark-matter, dark-energy, astro-biological system, possesses the attributes enabling life—predominantly water- and carbon-based—to flourish in its current phase.

Conflicts of Interest: The author declares no conflict of interest.

References

1. Weinberg, S. The cosmological constant problem. *Rev. Mod. Phys.***1989**, *61*, 1-23.
2. Martinez, R.; Agnihotri, A.N.; Boduch, Ph.; et al. Production of hydronium ion $(H_3O)^+$ and protonated water clusters $(H_2O)_{21}H^+$ after energetic ion bombardment of water ice in astrophysical environments. *J. Phys. Chem. A* **2019**, *123*, 8001-8008.
3. Badiei, S.; Holmlid, L. Rydberg matter in space: low-density condensed dark matter. *Mon. Not. R. Astron. Soc.* **2002**, *333*, 360-364.
4. Beck, C.; Mackey, M.C. Could dark energy be measured in the lab? *Phys. Lett. B* **2005**, *605*, 295-300; Measurability of vacuum fluctuations and dark energy. *Physica A* **2007**, *379*, 101-110.
5. Souza, R. D.; Impens, F.; Neto, P.A.M. Microscopic dynamical Casimir effect. *Phys. Rev. A* **2018**, *97*, 032514-032523.
6. Johnson, K. Terahertz vibrational properties of water nanoclusters relevant to biology. *J. Biol. Phys.* **2012**, *38*, 85-95.
7. Gilbert, W. The RNA world. *Nature* **1986**, *319*, 618.
8. Bergin, E.A.; van Dishoeck, E.F. Water in star- and planet-forming regions. *Phil. Trans. R. Soc.A* **2012**, *370*, 2778-2802.
9. Glanz, J.A. Water generator in the Orion nebula. *Science* **1998** *280*, 378-382.
10. Bradford, C.M.; Bolatto, A.D.; Maloney, P.R.; et al. The water vapor spectrum of APM 08279+5255: x-ray heating and infrared pumping over hundreds of parsecs. *ApJ* **2011**, *741*, L37-L43.
11. Bialy, S.; Sternberg, A.; Loeb, A. Water formation during the epoch of first metal enrichment. *ApJ* **2015**, *804*, L29-L34.
12. Aplin, K.L.; McPheat, R.A. Absorption of infra-red radiation by atmospheric molecular cluster-ions. *J. Atmos. Solar Terrest. Phys.* **2005**, *67*, 775-783.
13. Matsuura, M.; De Buizer, J.M.; Arendt, R.G.; et al. SOFIA mid-infrared observations of supernova 1987A in 2016 – forward shocks and possible dust re-formation in the post-shocked region. *Mon. Not. R. Astron. Soc.***2019,** *482*, 1715-1723.
14. Duley, W.W. Molecular clusters in interstellar clouds. *ApJ* **1996**, *471*, L57-L60.
15. Johnson, K.H.; Gallagher, M.P.; Mamer, O.; et al. Water vapor: an extraordinary terahertz wave source under optical excitation. *Phys. Lett. A* **2008**, *371*, 6037-6040.
16. Lis, D.C.; Schilke, P.; Bergin, E.A.; et al. Widespread rotationally hot hydronium ion in the galactic interstellar medium. *ApJ* **2014**, *785*, 135-144.
17. Slater, J.C.; Johnson, K.H. Self-consistent-field Xα cluster method for polyatomic molecules and solids. *Phys. Rev. B* **1972**, *5*, 844-853; Quantum chemistry and catalysis. *Physics Today* **1974**, *27*, 34-41.
18. Brudermann, J.; Lohbrandt, P.; Buck, U. Surface vibrations of large water clusters by He atom scattering. *Phys. Rev. Lett.* **1998,** *80*, 2821-2824.
19. Jordan, K. D. A fresh look at electron hydration. *Science* **2004**, *306*, 618-619.
20. Badiei, S.; Holmlid, L. Rydberg matter in space: low-density condensed dark matter. *Mon. Not. R. Astron. Soc.* **2002**, *333*, 360-364.
21. Van Dokkum, P.; Danieli, S.; Cohen, Y. ; et al. A galaxy lacking dark matter. *Nature* **2018**, *555*, 629–632.
22. Minami, Y.; Komatsu, E. New extraction of the cosmic birefringence from the Planck 2018 polarization data. *Phys. Rev. Lett.* **2020,** *125*, 221301-221317.
23. Diego-Palazuelos, P.; Eskilt, J.R.; Minami, Y.; et al. Cosmic birefringence from Planck data release 4. *Phys Rev Lett.* **2022,** *128*, 091302-091309.

24. Zhao, H.; Tan, Y.; Zhang, L.; et al. Ultrafast hydrogen bond dynamics of liquid water revealed by terahertz-induced transient birefringence. *Light Sci. Appl.* **2020, *9***, 136-139.
25. Clowe, D.; Gonzalez, A.; Markevich, A. Weak-lensing mass reconstruction of the interacting cluster 1E 0657-558: direct evidence for the existence of dark matter. *ApJ* **2004**, *604*, 596-604.
26. Munoz, J. B.; Loeb, A. A small amount of mini-charged dark matter could cool the baryons in the early universe, *Nature* **2018**, *557*, 684-686.
27. Sharma, G.; Salucci, P.; van de Ven, G.; Observational evidence of evolving dark matter profiles at $z \leq 1$. *A&A* **2022**, *659*, A40.
28. Weinberg, S. Anthropic bound on the cosmological constant. *Phys. Rev. Lett.* **1987**, *59*, 2607-2610.
29. Steinhardt, P. J. A quintessential introduction to dark energy. *Phil. Trans. R. Soc. Lond. A* **2003**, *361*, 2497-2513.
30. Guth, A. H. Inflationary universe: a possible solution to the horizon and flatness problems. *Phys. Rev. D* **1981**, *23*, 347-356; Eternal inflation and its implications. *J. Phys. A* **2007**, *30*, 6811-6826.
31. Layzer, D.; Hively, R. Origin of the microwave background. *ApJ* **1973**, *179*, 361-370.
32. Wright, E. L. Thermalization of starlight by elongated grains – could the microwave background have been produced by stars. *ApJ* **1982**, *255*, 401-407.
33. Lehnert, M.; Nesvadba, N.; Cuby, JG.; et al. Spectroscopic confirmation of a galaxy at redshift $z = 8.6$. *Nature* **2010,** *467*, 940–942.
34. Zheng, W.; Postman, M.; Zitrin, A.; et al. A magnified young galaxy from about 500 million years after the big bang. *Nature* **2012**, *489*, 406–408.
35. Oesch, P.A.; Brammer, G.; van Dokkum, P.G.; et al. A remarkably luminous galaxy at z = 11.1 measured with Hubble space telescope Grism spectroscopy. *ApJ* **2016**, *819*, 129-140.
36. Witze, A. Four revelations from the Webb telescope about distant galaxies. *Nature* **2022**, *608, 18-19.*
37. Vacher, L.; Aumont, J.; Boulanger, F.; et al. Frequency dependence of the thermal dust E/B ratio and EB correlation: insights from the spin-moment expansion. *A&A* **2023**, *672*, A146, 1-13.
38. Ade, P.A.R. ; Aghanim, N. ; Ahmed, Z. ; et al. Joint analysis of BICEP2/Keck array and Planck data. *Phys. Rev. Lett*. **2015,** *114*, 101301-101306.
39. Banandos, E.; Rauch, M.; Decarli, R.; et al. A metal-poor damped Lyα system at redshift 6.4. *ApJ* **2019**, *885*, 59-74.
40. Carlon, H.R. Infrared absorption by molecular clusters in water vapor. *J. Appl. Phys*.**1981**, *52*, 3111-3115.
41. Laporte, N.; Ellis, R.S.; Boone, F.; et al. Dust in the reionization era: ALMA observations of a $z = 8.38$ gravitationally lensed galaxy. *ApJL* **837**, *L21*, 1-6
42. Penrose, R. Before the big bang: an outrageous new perspective and its implications for particle physics. In: *Proceedings of EPAC 2006, Edinburgh, Scotland*. pp. 2759-2762.
43. Ijjas, A.; Steinhardt, P. J. A new kind of cyclic universe. *Phys. Lett. B* **2019**, *795*, 666-672.
44. Cleeves, L.I.; Bergin, E.A.; Alexander, C.M.O'D; et al. The ancient heritage of water ice in the solar system. *Science* **2014**, *345*, 1590-1593.
45. Kvenvolden**,** K.; Lawless**,** J.; Pering, K.; et al. Amino acids in the Murchison meteorite. *Nature* **1970**, *228*, 923-926.
46. Lacy, J.H.; Carr, J.S.; Evans, N.J.; et al. Discovery of interstellar methane – observations of gaseous and solid CH4 absorption toward young stars in molecular clouds. *ApJ*. **1991**, *376*, 556–560.
47. Iglesias-Groth S.; Manchado, A.; Rebolo, R. A. Search for interstellar anthracene towards the Perseus anomalous microwave emission region. *Mon. Not. R. Astron. Soc.* **2010**, *407*, 2157–2165.
48. Cotton, F.A.; Norman, J.G.; Johnson, K.H. Biochemical importance of the binding of phosphate by arginyl groups. Model compounds containing methylguanidinium ion. JACS **1973**, *95*, 2367–2369.
49. Yang, C.Y.; Johnson, K.H., Holm, R.H.; Norman J.G. Theoretical model for the 4-Fe active sites in oxidized ferredoxin and reduced high-potential proteins. Electronic structure of the analog $[FeS^*_4(SCH3)_4]^{4-}$. JACS **1975**, *97*, 6596–6598.
50. Case, D.A,; Huynh, B.H.; Karplus, M. Binding of oxygen and carbon monoxide to hemoglobin. An analysis of the ground and excited states. JACS **1979**, *101*, 4433–4453.
51. Joyce, G.F.; Orgel, L.E. Prospects for understanding the origin of the RNA world. In: Gesteland, R. F., Atkins, J. F., editors. *The RNA World*, Cold Spring Harbor Laboratory Press: Cold Spring Harbor, NY, 1993, pp. 1-22.
52. Costanzo, G.; Pino, S.; Cicinello, F.; et al. Generation of long RNA chains in water. *J. Biol. Chem.* **2009**, *284*, 33206–33216.
53. Cafferty, B. J.; Hud, N. V. Abiotic synthesis of RNA in water: a common goal of prebiotic chemistry and bottom-up synthetic biology, *Current Opinions in Chemical Biology* **2014**, *22*, 146-157.
54. Harker, H.A.; Viant, M.R.; Keutsch, F.N.; et al. Water pentamer: characterization of the torsional-puckering manifold by terahertz VRT spectroscopy. *J. Phys. Chem. A* **2005**, *109*, 6483–6497.
55. Teeter, M.M. Water Structure of a hydrophobic protein at atomic resolution: pentagon rings of water molecules in crystals of crambin, *Proc. Natl. Acad. Sci.* **1984**, *81*, 6014-6018.

56. Nandi, P.K.; Burnham, C.J.; Futera, Z.; et al. Ice-amorphization of supercooled water nanodroplets in no man's land. ACS Earth and Space Chemistry **2017**, *1*, 187–186.
57. Yokoyama, H.; Kannami, M.; Kanno, H. Intermediate range O-O correlations in supercooled water. *Chem. Phys. Lett.* **2008**, *463*, 99-102.
58. Sahle, C.J.; Sternemann, C.; Schmidt, C.; et al. Microscopic structure of water at elevated pressures and temperatures. ProNatl. Acad. Sci. **2013**, *110*, 6301–6306.
59. Bersuker, I.B.; Polinger, V.Z. *Vibronic Interactions in Molecules and Crystals*, Springer-Verlag: Berlin, 1989.
60. Meierhenrich, U.J ; Filippi, J.J.; Meinert, C..; et al. On the origin of primitive cells: from nutrient intake to elongation of encapsulated nucleotides. *Angew.Chem.Int.Ed.* **2010**, *49*, 3738-3750.
61. Dworkin, J.P.; Deamer, D.W.; Sandford, S.A.; et al. Self-assembling amphiphilic molecules: synthesis in simulated interstellar/precometary ices. *PNAS* **2001**, *98*, 815-819.
62. Chang, G.-G.; Huang, T.-M.; Hung, H.-C. Reverse micelles as life-mimicking systems. *Proc. Nat. Sci. Counc. ROC(B)* **2000**, *24*, 89-100.
63. Hanczyc, M.M.; Szostak, J.W. Replicating vesicles as models of primitive cell growth and division. *Current Opinions in Chemical Biology* **2004,** *8*, 660-664.
64. Milshteyn, D.; Milshteyn, D.; Damer, B. ; et al. Amphiphilic compounds assemble into membranous vesicles in hydrothermal hot spring water but not in seawater. *Life* **2018** *8*, 11-26.
65. Moelling, K. ; Broecker, F. Viruses and evolution – viruses first? A personal perspective. *Frontiers in Microbiology* **2019,** *10*, 1-13.
66. Kumar, A.; Blum, J.; Thanh Le, T. The mRNA vaccine development landscape for infectious diseases **2022**, *21*, 333-334.
67. Haynes, K. What is dark matter? Even the best theories are crumbling. *Discover Magazine* **2018**, September 21.
68. Heymans, C.; Van Waerbeke , L.; Miller, L.; et al. CFHTLenS: the Canada-France-Hawaii telescope lensing survey. *Mon. Not. R. Astron. Soc.* **2012**, *427*, 146-166.
69. Lockman, F.J.; Free, N.L.; Shields, J.C. The neutral hydrogen bridge between M31 and M33. *Astron. J.* **2012**, *144*, 52-59.
70. Cami, J. ; Bernard-Salas, J. ; Els Peeters, J.; ;et al. Detection of C60 and C70 in a young planetary nebula. *Science* **2010**, *329*, 1180-1182.
71. Coates, A. J.; **Wellbrock, A.; Jones, G.H.; et** al. Photoelectrons in the Enceladus plume. *J. Geophys. Res. Space Phys*. **2013**, *118*, 5099-5108.